3 Phenomenology of the Standard Model

With the discovery of the Higgs boson in 2012, the Standard Model may well be complete. More precisely, it may be that we know all nature's degrees of freedom up to energy scales of order one TeV and fully understand their interactions (there might be other degrees of freedom with couplings to quarks, leptons and gauge bosons which are significantly suppressed). The predictions of the Standard Model have been subjected to experimental tests in a broad range of processes. In experiments involving leptons alone, or hadrons at high-momentum transfers, detailed and precise predictions are possible. In processes involving hadrons at low momentum, it is often possible to make progress using symmetry arguments. In still other cases one can at least formulate a qualitative picture. In recent years, developments in lattice gauge theory have yielded reliable and precise predictions for at least some features of the large-distance behavior of hadrons. Since 2012 the Higgs boson itself has begun to provide a testing ground for many elements of the Standard Model. There exist excellent texts and reviews treating all these topics. Here we will give only a brief survey, attempting to introduce ideas and techniques which are important in understanding what may lie beyond the Standard Model.

3.1 The weak interactions

We are now in a position to describe weak interactions within the Standard Model. Summarizing our results for the W and Z masses, we have at tree level

$$M_W^2 = \frac{\pi\alpha}{\sqrt{2}G_{\rm F}\sin^2\theta_{\rm w}}, \quad M_Z^2 = \frac{\pi\alpha}{\sqrt{2}G_{\rm F}\sin^2\theta_{\rm w}\cos^2\theta_{\rm w}}, \tag{3.1}$$

where $\theta_{\rm w}$ is given by Eq. (2.84) and α is the fine-structure constant. Note in particular that, in the leading approximation,

$$\frac{M_W^2}{M_Z^2} = \cos^2\theta_{\rm w}. \tag{3.2}$$

In these expressions the Fermi constant is related to the W mass and the gauge coupling, through

$$G_{\rm F} = \sqrt{2}\frac{g^2}{8M_W^2}; \quad G_{\rm F} = 1.166 \times 10^{-5}\ {\rm GeV}^{-2}. \tag{3.3}$$

https://doi.org/10.1017/9781009290883.008 Published online by Cambridge University Press

The Weinberg angle $\theta_{\rm w}$ is given by

$$\sin^2\theta_{\rm w} = 0.231\,20(15). \tag{3.4}$$

The measured values of the W and Z masses are

$$M_W = 80.425(38)\ \text{GeV}, \quad M_Z = 91.1876(21)\ \text{GeV}. \tag{3.5}$$

One can see that the experimental quantities satisfy the theoretical relations to good accuracy. They are all in agreement at the one part in 10^2–10^3 level when radiative corrections are included.

The effective Lagrangian for the quarks and leptons obtained by integrating out the W and Z particles is

$$\mathcal{L}_W + \mathcal{L}_Z = \frac{8G_{\rm F}}{\sqrt{2}}\left[\left(J^1_\mu\right)^2 + \left(J^2_\mu\right)^2 + \left(J^3_\mu - \sin^2\theta_{\rm w} J_{\mu\rm EM}\right)^2\right]. \tag{3.6}$$

The first two terms correspond to the exchange of the charged $W^\pm$ fields. The last term represents the effect of Z boson exchange. This structure has been tested extensively.

The most precise tests of the weak interaction theory involve the Z bosons. Experiments at the LEP accelerator at CERN and the SLD accelerator at SLAC produced millions of Z bosons. These large samples permitted high-precision studies of the line shape and of the branching ratios to various final states. Care is needed in calculating the radiative corrections; it is important to make consistent definitions of the various quantities. Detailed comparisons of theory and experiment can be found on the website of the Particle Data Group (http://pdg.lbl.gov). As inputs, one generally takes the value of $G_{\rm F}$ measured in μ decays, the measured mass of the Z and the fine structure constant. Outputs include the Z boson total width:

$$\text{experiment, } \Gamma_Z = 2.4952 \pm 0.0023; \quad \text{theory, } \Gamma_Z = 2.4955 \pm 0.0009. \tag{3.7}$$

The decay width of the Z to hadrons and leptons is also in close agreement (see Fig. 3.1). The W mass can also be computed with the above inputs and has been measured quite precisely, particularly at the Tevatron and LEP2 (below we quote first the LEP result and then the Tevatron result):

$$\begin{aligned} \text{experiment, } M_W &= 80.376 \pm 0.033,\ 80.387 \pm 0.016 \pm 0.0023; \\ \text{theory, } M_W &= 80.363 \pm 0.06. \end{aligned} \tag{3.8}$$

The W width, similarly, is:

$$\begin{aligned} \text{experiment, } \Gamma_W &= 2.196 \pm 0.083,\ 2.046 \pm 0.0049; \\ \text{theory } \Gamma_W &= 2.090 \pm 0.001. \end{aligned} \tag{3.9}$$

https://doi.org/10.1017/9781009290883.008 Published online by Cambridge University Press

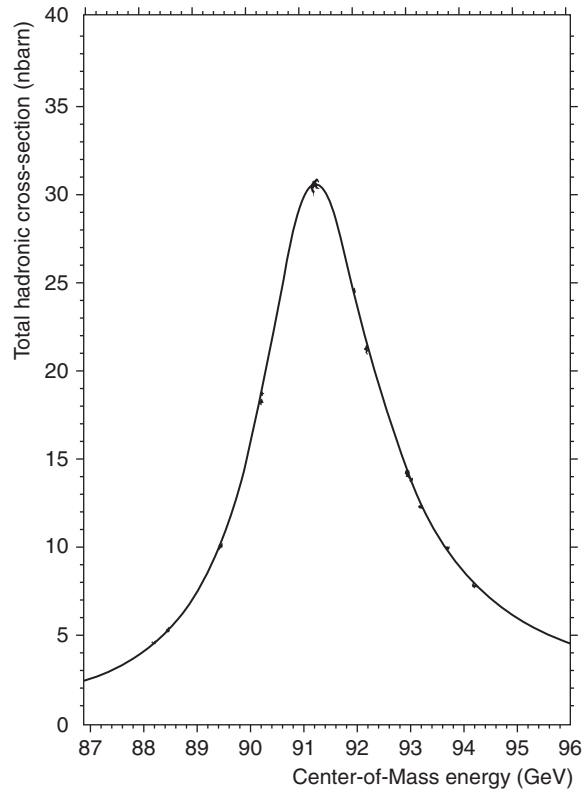

Fig. 3.1 OPAL results for the Z line shape. The solid line corresponds to the theory; the dots give the data.

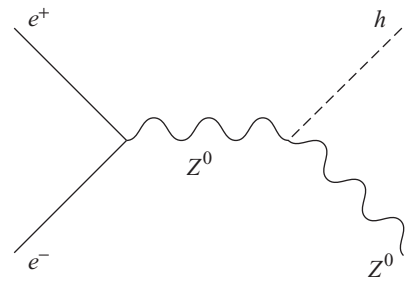

Fig. 3.2 The Higgs can be produced in e^+e^- annihilation, in association with a Z^0 particle.

3.2 Discovery of the Higgs

The simplest possible realization of the Higgs mechanism within the Standard Model is through a single Higgs doublet. In 2012 the two large detectors at the Large Hadron Collider, ATLAS and CMS, reported the discovery of a scalar particle behaving like the Higgs field of this minimal model. The mass of this particle is 125.6 ± 0.4 GeV. As we

https://doi.org/10.1017/9781009290883.008 Published online by Cambridge University Press

will explain in a bit more detail shortly, as of this writing both the production cross section and the decays of the Higgs are in rough agreement (10%−20% for several channels) with Standard Model predictions. The precision of these measurements and the quality of Standard Model tests will improve over the next few years. Any model for physics beyond the Standard Model must reproduce these features. It is likely (as we will discuss in the next chapter) that there is a range of energies where the Standard Model is completely described by the Lagrangian of the previous chapter.

3.2.1 Testing the Standard Model with the Higgs

The discovery of the Higgs boson, exciting in itself, brought together many aspects of the Standard Model. The Higgs was discovered in high-energy proton–proton collisions, and understanding the signal requires the full machinery of perturbative QCD (which we will review shortly) including parton distribution functions and higher-order radiative corrections. Higgs production arises through processes including *gluon fusion* (Fig. 3.3), the collision of a gluon from each of the two protons to produce a virtual top quark pair, which then couples to the Higgs, as well as a smaller contribution from quark collisions. There is an equally rich story with the decay channels. Large numbers of Higgs particles are produced at the LHC. The Higgs decays predominantly to $b\bar{b}$ pairs, however, and it is difficult to isolate these decays from the many other sources of such pairs in proton collisions. The original discovery was made in the two-photon channel, whose branching ratio is far smaller but where it is easier (but still challenging) to separate the signal from the background. Indeed, a simple-minded estimate suggests the branching ratio should be of an order given by

$$\frac{\Gamma(H \to \gamma\gamma)}{\Gamma(H \to b\bar{b})} \sim \left(\frac{\alpha}{4\pi}\right)^2 \frac{m_H^3 v^2}{m_t^2 m_b^2} \approx 10^{-4}. \tag{3.10}$$

Comparisons of theory and experiment in the two-photon channel are indicated in Figs. 3.4 and 3.5. Other channels in which comparisons can be made, as of the time of writing,

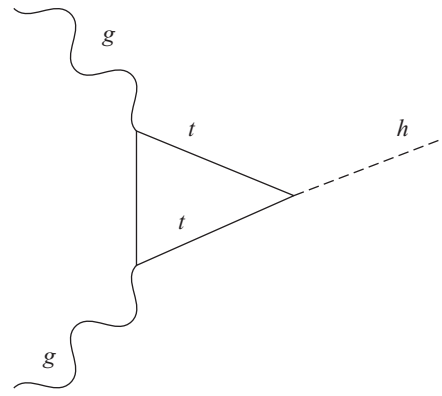

Fig. 3.3 In hadron colliders Higgs particles can be produced by several mechanisms. The diagram above illustrates production by gluons.

https://doi.org/10.1017/9781009290883.008 Published online by Cambridge University Press

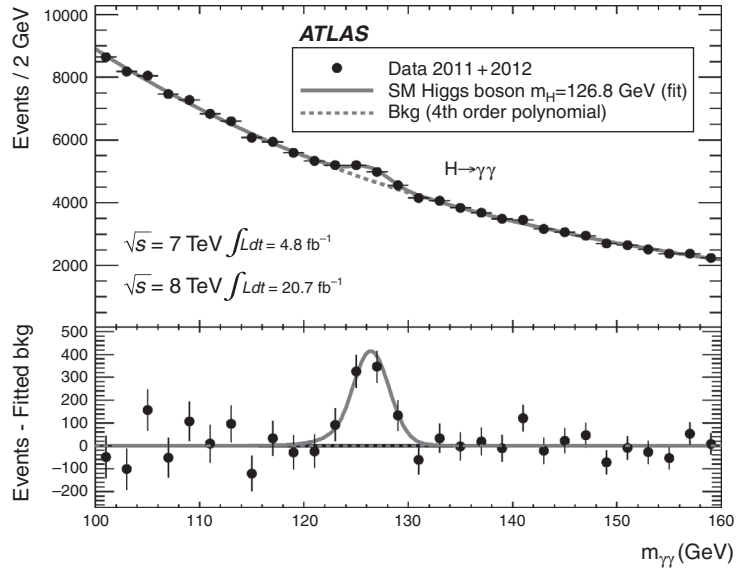

Fig. 3.4 ATLAS data on two-photon production.

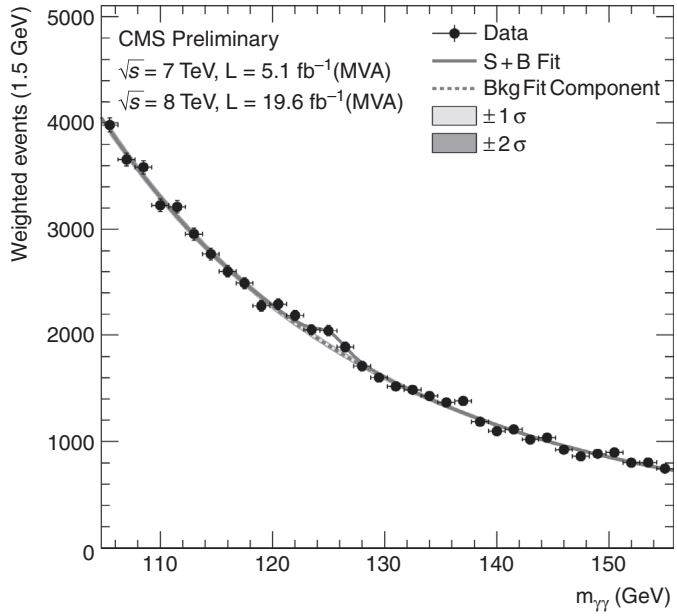

Fig. 3.5 CMS data on two-photon production.

are the *ZZ* channel (with four observed leptons from the *Z* decays) and the *WW* channel. Comparisons, again, with Standard Model expectations appear in Fig. 3.6.

Future runs of the LHC, with higher energies and higher luminosities, will increase the precision of these studies, in many cases at the 5% – 10% level. An electron–positron linear

https://doi.org/10.1017/9781009290883.008 Published online by Cambridge University Press

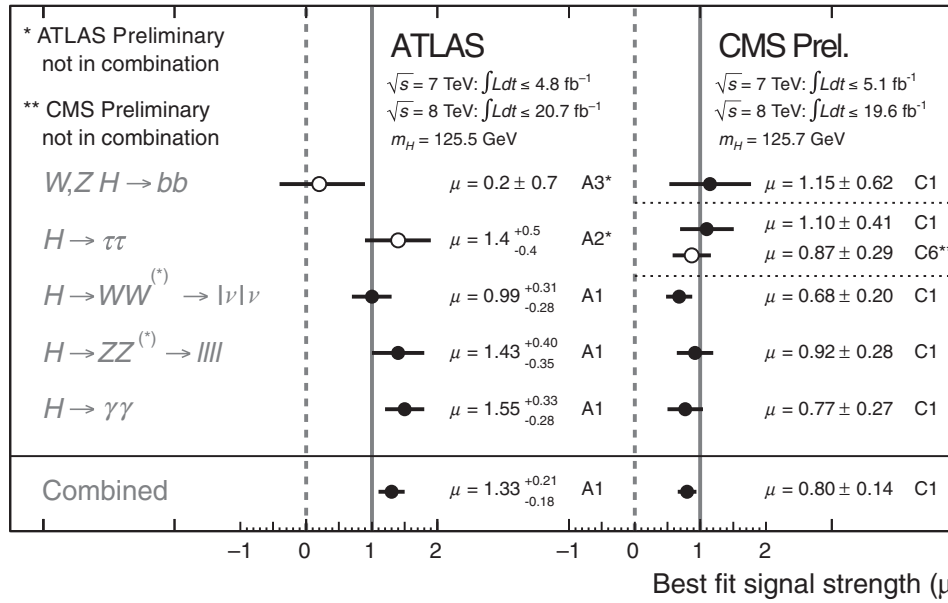

Fig. 3.6 For comparison, ATLAS and CMS measurements of Higgs, in several channels. Used by permission of the Particle Data Group.

collider, or other contemplated high-energy lepton machines, could improve the precision to the few percent level.

In any case, at present it appears that the Standard Model may be complete; any degrees of freedom in nature beyond those of the theory may well be significantly heavier than the Higgs. This clearly has implications for the possible physics we might hope to see beyond the Standard Model. We will discuss this further when we consider supersymmetric models, which predict multiple Higgs doublets.

3.3 The quark and lepton mass matrices

Before considering the small neutrino masses, we note that the lepton–Yukawa couplings can simply be taken as diagonal: there is no mixing. Their extraction from the experimental data is reasonably straightforward. The lepton masses are

$$m_e = 0.511 \text{ MeV}, \quad m_\mu = 113 \text{ MeV}, \quad m_\tau = 1.777 \text{ GeV}. \tag{3.11}$$

The quark masses and mixings pose more severe challenges. First, there is the question of mixing. We have seen that we can take the Yukawa coupling y_u for the u quarks to be diagonal, but we cannot simultaneously diagonalize the couplings y_d for the d quarks. As a result, when the Higgs field acquires an expectation value v, the u quark masses are

https://doi.org/10.1017/9781009290883.008 Published online by Cambridge University Press

given by

$$m_{uf} = \frac{(y_u)_f}{\sqrt{2}} v. \tag{3.12}$$

These are automatically diagonal. But the d quark masses are described by a 3×3 mass matrix,

$$m_{d\,ff'} = \frac{(y_d)_{ff'}}{\sqrt{2}} v. \tag{3.13}$$

We can diagonalize this matrix by separate unitary transformations of the $\bar{d}$ and d fields. Because the $\bar{d}$ quarks are singlets of $SU(2)$, the transformation of the $\bar{d}$ field leaves the kinetic terms and gauge interactions for these quarks unchanged. But the transformation for the d quarks does not commute with $SU(2)$, so the couplings of the gauge bosons to these quarks are more complicated. The unitary transformation between the mass or flavor eigenstates and the weak interaction eigenstates is known as the CKM matrix. Denoting the mass eigenstates as u', d', etc., the transformation has the form

$$\begin{pmatrix} d' \\ s' \\ b' \end{pmatrix} = \begin{pmatrix} V_{ud} & V_{us} & V_{ub} \\ V_{cd} & V_{cs} & V_{cb} \\ V_{td} & V_{ts} & V_{tb} \end{pmatrix} \begin{pmatrix} d \\ s \\ b \end{pmatrix}. \tag{3.14}$$

There are various ways of parameterizing the CKM matrix. One standard form, which makes its unitarity manifest, is given as follows:

$$V = \begin{pmatrix} c_{12}c_{13} & s_{12}c_{13} & s_{13}e^{-i\delta} \\ -s_{12}c_{23} - c_{12}s_{23}s_{13}e^{i\delta} & c_{12}c_{23} - s_{12}c_{23}s_{13}e^{i\delta} & s_{23}c_{13} \\ s_{12}s_{23} - c_{12}c_{23}s_{13}e^{i\delta} & -c_{12}s_{23} - s_{12}c_{23}s_{13}e^{i\delta} & c_{23}c_{13} \end{pmatrix}. \tag{3.15}$$

The matrix V is real unless δ is non-zero. Thus δ provides a measure of CP violation.

Experimentally, all the off-diagonal matrix elements are small and in fact are hierarchically so. Wolfenstein developed a convenient parameterization:

$$V = \begin{pmatrix} 1 - \lambda^2/2 & \lambda & A\lambda^3(\rho - i\eta) \\ -\lambda & 1 - \lambda^2/2 & A\lambda^2 \\ A\lambda^3(1 - \rho - i\eta) & -A\lambda^2 & 1 \end{pmatrix} + \mathcal{O}(\lambda^4). \tag{3.16}$$

The Babar and Belle experiments improved significantly our knowledge of these quantities, and in particular of the CP-violating parameter. They demonstrated that, indeed, V is nearly unitary, which constrains possible new physics. The magnitudes of the matrix elements of V are as follows:

$$V = \begin{pmatrix} 0.974\,27 \pm 0.0014 & 0.225\,36 \pm 0.000\,61 & 0.003\,55 \pm 0.000\,15 \\ 0.225\,22 \pm 0.000\,61 & 0.973\,43 \pm 0.000\,15 & 0.0414 \pm 0.0012 \\ 0.008\,86^{+0.000\,33}_{-0.000\,32} & 0.0405^{+0.000\,11}_{-0.000\,12} & 0.999\,14 \pm 0.0005 \end{pmatrix}. \tag{3.17}$$

The Wolfenstein parameters are

$$\begin{aligned} \lambda &= 0.225\,37 \pm 0.000\,61, \quad A = 0.814^{+0.023}_{-0.024,} \\ \bar{\rho} &= 0.117 \pm 0.021, \quad \bar{\eta} = 0.353 \pm 0.013. \end{aligned} \tag{3.18}$$

https://doi.org/10.1017/9781009290883.008 Published online by Cambridge University Press

(Here we are following the conventions of the Particle Data Group; $\bar{\rho} = \rho(1 - \lambda^2/2)$.) Note, in particular, that the CP-violating parameter $\bar{\eta}$ is not small (corresponding to δ of order one).

From unitarity follow a number of relations among the elements of the matrix. For example,

$$V_{ud}V_{ub}^* + V_{cd}V_{cb}^* + V_{td}V_{tb}^* = 0. \tag{3.19}$$

From $V_{ud} \approx V_{cb} \approx V_{tb} \approx 1$, this becomes a relation between three complex numbers which says that they form a triangle the *unitarity triangle*. Determining from experiment that these quantities do indeed form a triangle is an important test of this model for the quark masses.

We should also discuss the values of the quark masses themselves. This is somewhat subtle, since we do not observe free quarks; the masses are Lagrangian parameters, related to experimental quantities in a way which depends on a scheme (i.e. a definition) and an energy scale, much as one must specify the scheme and energy scale of the gauge coupling in QCD. For the lighter quarks (u, d and s) these masses can be obtained, at present, only from lattice QCD. As we will discuss further in Section 3.8 on lattice gauge theory, this is a subtle and complex process. However, over the past decade, reliable computations have become possible, with errors at the level of 10% or smaller. With a scale of order 2 GeV, in the $\overline{MS}$ scheme the Particle Data Group, combining results from different lattice collaborations, quotes the following quark masses:

$$\begin{aligned} m_u &= 2.15(15)\ \text{MeV}, \quad m_d = 4.7(20)\ \text{MeV}, \quad m_s = 93.5(2.5)\ \text{MeV}, \\ m_c &\approx 1.15{-}1.35\ \text{GeV}, \quad m_b \approx 4.1{-}4.4\ \text{GeV}, \quad m_t \approx 174.3 \pm 5\ \text{GeV}. \end{aligned} \tag{3.20}$$

Overall, the picture of the quark and lepton masses is quite puzzling. They vary over nearly five orders of magnitude. Correspondingly, the dimensionless Yukawa couplings have widely disparate values. At the same time the mixing among the quarks is small and hierarchical. Understanding these features might well be a clue to what lies beyond the Standard Model.

We will discuss the question of neutrino masses in Chapter 4, when we discuss the Standard Model as an effective field theory, and in particular the non-renormalizable operators which might arise from integrating out the Beyond the Standard Model physics. We will see that the pattern of neutrino masses does not resemble that of the quarks and charged leptons; they appear anarchical, rather than hierarchical.

3.4 The strong interactions

The strong interactions, as their name implies, are characterized by strong coupling. As a result, perturbative methods are not suitable for most questions. In comparing theory and experiment it is necessary to focus on a few phenomena which are accessible to theoretical analysis. By itself this is not particularly disturbing. A parallel with the quantum mechanics of electrons interacting with nuclei is perhaps helpful. We can understand simple atoms

https://doi.org/10.1017/9781009290883.008 Published online by Cambridge University Press

in detail; atoms with very large Z can be treated by Hartree–Fock or other methods. Atoms with intermediate Z, however, can be dealt with only by, at best, detailed numerical analysis accompanied by educated guesswork. Molecules are even more problematic, not to mention solids. But we are able to make detailed tests of the theory (and its extension in quantum electrodynamics) from the simpler systems, and develop a qualitative understanding of the more complicated systems. In many cases we can do a quantitative analysis of small fluctuations about the ground states of the complicated system.

In the theory of strong interactions, as we will see, many problems are hopelessly complicated. Low-lying spectra are hard to deal with; detailed exclusive cross sections in high-energy scattering are essentially impossible. There are many questions we can answer, though. Rates for inclusive questions at very high energy and momentum transfer can be calculated with high precision. Qualitative features of the low-lying spectra of hadron systems and their interactions at low energies can be understood in a qualitative (and sometimes quantitative) fashion by symmetry arguments. Such systems include those in which heavy quarks are bound to light quarks. Recently, progress in lattice gauge theory has made it possible to perform calculations which previously seemed impossible, for features of spectra and even for interaction rates that are important for understanding weak interactions.

3.4.1 Asymptotic freedom

The coupling of a gauge theory (and more generally of a field theory) is a function of energy or length scale. If a typical momentum transfer in a process is q, and if M denotes the cutoff scale, then

$$\frac{8\pi^2}{g^2(q^2)} = \frac{8\pi^2}{g^2(M)} + b_0 \ln \frac{q^2}{M^2}. \tag{3.21}$$

Here

$$b_0 = \frac{11}{3} C_{\mathrm{A}} - \frac{2}{3} c_i n_f^{(i)} - \frac{1}{3} c_i n_\phi^{(i)}. \tag{3.22}$$

In this expression $n_f^{(i)}$ is the number of left-handed fermions in the ith representation, while $n_\phi^{(i)}$ is the number of scalars; C_{A} is the quadratic Casimir operator of the adjoint representation and c_i is the quadratic Casimir operator of the ith representation. Thus

$$f^{acd} f^{bcd} = C_{\mathrm{A}} \delta^{ab}, \quad \mathrm{Tr}(T^a T^b) = c_i \delta^{ab}. \tag{3.23}$$

These formulas are valid if the masses of the fermions and scalars are negligible at scale q^2. For example, in QCD, at scales of order the Z boson mass, the masses of all but the top quark can be neglected. All the quarks are in the fundamental representation, and there are no scalars. So $b_0 = 22/3$. As a result, g^2 gets smaller as q^2 gets larger and, conversely, g^2 gets larger as q^2 gets smaller. Since momentum transfer is inversely proportional to a typical distance scale, one can say that the strong force gets weaker at short distances, and stronger at large distances. We will calculate b_0 in Section 3.5.

https://doi.org/10.1017/9781009290883.008 Published online by Cambridge University Press

This is quite striking. In the case of QCD it means that hadrons, when probed at very large momentum transfer, behave as collections of free quarks and gluons. Perturbation theory can be used to make precise predictions. However, viewed at large distances hadrons are strongly interacting entities. Perturbation theory is not a useful tool, and other methods must be employed. The most striking phenomena in this regime are confinement – the fact that one cannot observe free quarks – and, closely related, the existence of a mass gap. Neither of these phenomena can be observed in perturbation theory.

3.5 The renormalization group

In thinking about physics beyond the Standard Model, by definition we are considering phenomena involving degrees of freedom to which we have, as yet, no direct experimental access. The question of degrees of freedom which are as yet unknown is the heart of the problem of renormalization. In the early days of quantum field theory it was often argued that one should be able to take a formal limit of infinite cutoff, $\Lambda \to \infty$. Ken Wilson promulgated a more reasonable view: real quantum field theories describe physics below some characteristic scale Λ. In a condensed matter system this might be the scale of the underlying lattice, below which the system may often be described by a continuum quantum field theory. In the Standard Model, a natural scale is the scale of the W and Z bosons. Below this scale the system can be described by a renormalizable field theory, QED plus QCD, along with certain non-renormalizable interactions – the four-fermion couplings of the weak interactions. In defining this theory, one can take the cutoff to be, say, M_W, or aM_W for some $a < 1$. Depending on the choice of a, the values of the couplings will vary. The parameters of the low-energy effective Lagrangian must depend on a in such a way that physical quantities are independent of this choice. The process of determining the values of couplings in an effective theory which reproduce the effects of some more microscopic theory is often referred to as *matching*.

Knowing how physical couplings depend on the cutoff, one can determine how physical quantities behave in the long-wavelength, infrared, regime by simple dimensional analysis. Quantities associated with operators of dimension less than four will grow in the infrared. They are said to be *relevant*. Those with dimension four will vary as powers of logarithms; they are said to be *marginal*. Quantities with dimension greater than four, those conventionally referred to as non-renormalizable operators, will become less and less important as the energy is lowered. They are said to be *irrelevant.* In strongly interacting theories, the dimensions of operators can be significantly different than those expected from naive classical considerations. The classification of operators as relevant, marginal, or irrelevant applies to their quantum behavior.

At sufficiently low energies we can ignore the irrelevant, non-renormalizable, couplings. Alternatively, by choosing the matching scale M to be low enough, only the marginal and relevant couplings will be important. In a theory with only dimensionless couplings, the variation of the coupling with q^2 is closely related to its variation with the cutoff, M. Physical quantities are independent of the cutoff, so any explicit dependence on the cutoff

https://doi.org/10.1017/9781009290883.008 Published online by Cambridge University Press

must be compensated by the dependence of the couplings on M. On dimensional grounds M^2 must appear with q^2, so a knowledge of the dependence of couplings on M permits a derivation of their dependence on q^2. More precisely, in studying, say, a cross section, any explicit dependence on the cutoff must be compensated by a dependence of the coupling on the cutoff. Calling the cross section or other physical quantity σ, we can express this dependence as a differential equation, the *renormalization group equation*:

$$\left(M\frac{\partial}{\partial M}+\beta(g)\frac{\partial}{\partial g}\right)\sigma=0. \tag{3.24}$$

Here the beta function (or β-function) is given by

$$\beta(g)=M\frac{\partial}{\partial M}g. \tag{3.25}$$

We can evaluate the beta function from our explicit expression, Eq. (3.21), for g^2:

$$\beta(g)=-b_0\frac{g^2}{16\pi^2}g. \tag{3.26}$$

We will compute b_0 in the next section. This equation has corrections in each order of perturbation theory and non-perturbative corrections as well.

So far we have expressed the coupling in terms of a cutoff and a physical scale. In old-fashioned language, the coupling $g^2(M)$ is the "bare" coupling. We can define a "renormalized coupling" $g^2(\mu)$ at a scale μ^2:

$$\frac{8\pi^2}{g^2(\mu^2)}=\frac{8\pi^2}{g^2(M)}+b_0\ln\frac{\mu}{M}. \tag{3.27}$$

In practice it is necessary to give a more precise definition. We will discuss this when we compute the beta function in the next section. Because of this need to give a precise definition of the renormalized coupling, care is required in comparing theory and experiment. As we will review shortly, there is a variety of definitions in common use and it is important to be consistent.

Quantities like Green's functions are not physical, and obey an inhomogeneous equation. One can obtain this equation in a variety of ways. For simplicity, consider first a Green's function with n scalar fields, such as

$$G(x_1,\ldots,x_n)=\langle\phi(x_1)\cdots\phi(x_n)\rangle. \tag{3.28}$$

This Green's function is related to the *renormalized* Green's function as follows. If the theory is defined at a scale μ, the effective Lagrangian takes the form

$$\mathcal{L}_\mu=Z^{-1}(\mu)(\partial_\mu\phi^2)+\cdots. \tag{3.29}$$

Here the factor Z^{-1} arises from integrating out the physics above the scale μ. It will typically include ultraviolet-divergent loop effects. Rescaling ϕ in such a way that the kinetic term is canonical, $\phi=Z^{1/2}\phi_{\rm r}$, we have that

$$G(x_1,\ldots,x_n)=Z(\mu)^{n/2}G_{\rm r}(x_1,\ldots,x_n). \tag{3.30}$$

https://doi.org/10.1017/9781009290883.008 Published online by Cambridge University Press

The left-hand side is independent of μ, so we can write an equation for $G_{\rm r}$,

$$\left(\mu\frac{\partial}{\partial\mu}+\beta(g)\frac{\partial}{\partial g}+n\gamma\right)G_{\rm r}=0, \tag{3.31}$$

where γ, known as the *anomalous dimension*, is given by

$$\gamma=\frac{1}{2}\mu\frac{\partial}{\partial\mu}\ln Z. \tag{3.32}$$

If these are several different fields, e.g. gauge fields, fermions and scalars, this equation is readily generalized. There is an anomalous dimension for each field, and the $n\gamma$ term is replaced by the appropriate number of fields of each type and their anomalous dimensions.

The effective action obeys a similar equation. Starting with

$$\Gamma(x_1,\ldots,x_n)=Z(\mu)^{-n/2}\Gamma_{\rm r}(x_1,\ldots,x_n), \tag{3.33}$$

we have

$$\left(\mu\frac{\partial}{\partial\mu}+\beta(g)\frac{\partial}{\partial g}-n\gamma\right)\Gamma_{\rm r}=0, \tag{3.34}$$

These equations are readily solved. We could write down the solution immediately, but an analogy with the motion of a fluid is helpful. A typical equation, for example, for the density of a component of a fluid (e.g. the density of bacteria in the fluid) would take the form

$$\left[\frac{\partial}{\partial t}+v(x)\frac{\partial}{\partial x}-\rho(x)\right]D(t,x)=0, \tag{3.35}$$

where $D(t,x)$ is the density as a function of position and time and $v(x)$ is the velocity of the fluid at x; ρ represents a source term (e.g. the growth due to the presence of yeast or a variable temperature). To solve this equation one first solves for the motion of an element of fluid initially at x, i.e. one solves:

$$\frac{d}{dt}\bar{x}(t;x)=v(\bar{x}(t;x)),\quad \bar{x}(0;x)=x. \tag{3.36}$$

In terms of $\bar{x}$ we can immediately write down a solution for D:

$$\begin{aligned}D(t,x)&=D_0(\bar{x}(t;x))\exp\left[\int_0^t dt'\,\rho(\bar{x}(t';x))\right]\\&=D_0(\bar{x}(t;x))\,\exp\left[\int_{\bar{x}(t)}^{x}dx'\frac{\rho(x')}{v(x')}\right].\end{aligned} \tag{3.37}$$

Here D_0 is the initial density. One can check this solution by plugging it into Eq. (3.35) directly, but each piece has a clear physical interpretation. For example, if there were no source ($\rho=0$), the solution would become $D_0(\bar{x}(t;x))$. With no velocity, the source would lead to just the expected growth in the density.

Let us apply this to Green's functions. Consider, for example, a two-point function, $G(p)=p^{-2}ih(p^2/\mu^2)$. In our fluid dynamics analogy the coupling g is the analog of the

https://doi.org/10.1017/9781009290883.008 Published online by Cambridge University Press

velocity; the log of the scale, $t = \ln(p/\mu)$, plays the role of the time. The equation for g is then

$$\left[\frac{\partial}{\partial t} - \beta(g)\frac{\partial}{\partial g} - 2\gamma(g)\right] h(t) = 0. \tag{3.38}$$

Define $\bar{g}(\mu)$ as the solution of

$$\mu\frac{\partial}{\partial \mu}\bar{g}(\mu) = \beta(\bar{g}). \tag{3.39}$$

At lowest order, this is solved by Eq. (3.27). Then

$$h(p,g) = h(\bar{g}(t)) \exp\left[2\int_{t_0}^{t} dt' \frac{\gamma(\bar{g}(t',g))}{\beta(\bar{g}(t',g))}\right]. \tag{3.40}$$

One can write the solution in the form

$$G(p,\lambda) = \frac{i}{p^2} G(\bar{g}(t;g)) \exp\left[2\int_{g}^{\bar{g}} dg' \frac{\gamma(g')}{\beta(g')}\right]. \tag{3.41}$$

3.6 Calculating the beta function

In the previous section we presented the one-loop result for the beta function and used it in various applications. In this section we actually compute this result. There are a number of ways to determine the variation of the gauge coupling with energy scale. One way is to calculate the potential for a very heavy quark–antiquark pair as a function of their separation R (we use the term quark here loosely for a field in the N-dimensional, or *fundamental*, representation of $SU(N)$). The potential is a renormalization-group-invariant quantity. At lowest order it is given by

$$V(R) = -\frac{g^2 C_{\mathrm{F}}}{R} \tag{3.42}$$

where

$$C_{\mathrm{F}} = \sum_{a=1}^{N^2-1} T^a T^a; \tag{3.43}$$

here C_{F} refers to the fundamental representation and T refers to the adjoint representation. The potential is a physical quantity; as a result it is renormalization-group invariant. In perturbation theory it has corrections behaving as $g^2(\mu)\ln(R\Lambda)$. This follows simply from dimensional analysis. So, if we choose $R = \mu^{-1}$ then the logarithmic terms disappear and we have

$$V(R) = -g^2(R)\frac{C_{\mathrm{F}}}{R}\left[1 + \mathcal{O}(g^2(R))\right]. \tag{3.44}$$

In an asymptotically free theory such as QCD, where the coupling gets smaller with distance, Eq. (3.41) becomes more and more reliable as R gets smaller. This result has

https://doi.org/10.1017/9781009290883.008 Published online by Cambridge University Press

physical applications. In the case of a bound state of a top quark and antiquark, one might hope that this would be a reasonable approximation and would describe the binding of the system. Taking $\alpha_s(R) \sim 0.1$, for example, would give a typical radius of order $(17\ \text{GeV})^{-1}$, a length scale where one might expect perturbation theory to be reliable (and for which $\alpha_s(R) \sim 0.1$). By analogy with the hydrogen atom, one would expect the binding energy to be of order 2 GeV. In practice, however, this is not directly relevant, since the width of the top quark is of the same order: the top quark decays before it has time to form a bound state. Still, it should be possible to see evidence for such QCD effects in the production of $t\bar{t}$ pairs near the threshold in e^+e^- annihilation.

A second approach is to study Green's functions in momentum space. The calculation is straightforward, if slightly more tedious than the analogous calculation in a $U(1)$ gauge theory (QED). The main complication is the three-gauge-boson vertex, which has many terms (at one loop, one can use symmetries to simplify greatly the algebra). It is necessary to have a suitable regulator for the integrals. By far the most efficient is the dimensional regularization technique of 't Hooft and Veltman. Here one initially allows the space–time dimensionality d to be arbitrary and takes $d \to 4-\epsilon$. For convenience, we include the two most frequently needed integration formulas below; their derivation can be found in many textbooks.

$$\int \frac{d^d k}{(k^2+M^2)^n} = \frac{\pi^{d/2}\Gamma(n-d/2)}{\Gamma(n)}(M^2)^{d/2-n}, \tag{3.45}$$

$$\int \frac{d^d k\, k^2}{(k^2+M^2)^n} = \frac{\pi^{d/2}\Gamma(n-d/2-1)}{\Gamma(n)}(M^2)^{d/2-n+1}. \tag{3.46}$$

Ultraviolet divergences, such as would occur for $n = 2$ in the first integral, give rise to poles in the limit $\epsilon \to 0$. If we were simply to cut off the integral at $k^2 = \Lambda^2$, we would find

$$\int \frac{d^4 k}{(2\pi)^4} \frac{1}{(k^2+M^2)^2} \approx \frac{1}{16\pi^2} \ln \frac{\Lambda}{M}. \tag{3.47}$$

In dimensional regularization this behaves as follows:

$$\int \frac{d^4 k}{(2\pi)^4} \frac{1}{(k^2+M^2)^2} = \frac{1}{16\pi^2}\Gamma\left(\frac{\epsilon}{2}\right) \approx \frac{1}{8\pi^2\epsilon}. \tag{3.48}$$

So ϵ should be thought of as $\ln \Lambda^2$. The computation of the Yang–Mills beta function by studying momentum-space Feynman diagrams can be found in many textbooks and is outlined in the exercises at the end of the chapter.

Here we follow a different approach, known as the background field method. This technique is closely tied to the path integral, which will play an important role in this book. It is also closely tied to the Wilsonian view of renormalization. We break up a field A into a long-wavelength part $\mathcal{A}$ and a shorter-wavelength, fluctuating, quantum part a:

$$A^\mu = \mathcal{A}^\mu + a^\mu. \tag{3.49}$$

We can think of $\mathcal{A}^\mu$ as corresponding to modes of the field with momenta below the scale q and a^μ as corresponding to higher momenta. We wish to compute an effective action

https://doi.org/10.1017/9781009290883.008 Published online by Cambridge University Press

for $\mathcal{A}^\mu$, integrating out the high-momentum modes:

$$\int [d\mathcal{A}] \int [da]\, e^{iS(\mathcal{A},a)} = \int [d\mathcal{A}]\, e^{iS_{\text{eff}}(\mathcal{A})}; \tag{3.50}$$

(see Appendix C for an explanation of the terminology). In calculating the effective action we are treating $\mathcal{A}^\mu$ as a fixed, classical, background. In this approach one can work entirely in Euclidean space, which greatly simplifies the calculation.

Our first task is to write down $e^{iS(\mathcal{A},a)}$. For this purpose, it is convenient to suppose that $\mathcal{A}$ satisfies its equation of motion. (Otherwise, it is necessary to introduce a source for a.) A convenient choice of gauge is known as the background field gauge,

$$D_\mu a^\mu = 0, \tag{3.51}$$

where D_μ is the covariant derivative defined with respect to the background field $\mathcal{A}$. At one loop we only need to work out the action to second order in the fluctuating fields a^μ, ψ, ϕ. Consider, first, the fermion action. To quadratic order we can set $a^\mu = 0$ in the Dirac Lagrangian. The same holds for scalars. So from the fermions and scalars we obtain

$$\det(\not{D})^{n_f} \det(D^2)^{-n_\phi/2}. \tag{3.52}$$

The fermion functional determinant can be greatly simplified; it is convenient, for this computation, to work with four-component Dirac fermions. Then

$$\begin{aligned} \det(\not{D}) &= \det(\not{D}\not{D})^{1/2} \\ &= \det\left(D^2 + \frac{1}{2} D_\mu D_\nu [\gamma^\mu, \gamma^\nu]\right) \\ &= \det(D^2 + \mathcal{F}^{\mu\nu}\mathcal{J}_{\mu\nu}). \end{aligned} \tag{3.53}$$

Here $\mathcal{F}^{\mu\nu}$ is the field strength associated with $\mathcal{A}$ (we have used the connection between the field strength and the commutator of covariant derivatives, Eq. (2.14)) and $\mathcal{J}_{\mu\nu}$ is the generator of Lorentz transformations in the fermion representation.

What is interesting is that we can write the gauge boson determinant, in the background field gauge, in a similar fashion.[1] With a little algebra, the gauge part of the action can be shown to be

$$\mathcal{L}_{\text{gauge}} = -\frac{1}{4g^2}\left(\text{Tr}\, \mathcal{F}^{a\,2}_{\mu\nu} - 2g^2 a^a_\mu D^2 a^{\mu\, a} - 2a^a_\mu f^{abc} \mathcal{F}^{b\mu\nu} a^c_\nu\right). \tag{3.54}$$

Here we have used the A^a_μ notation in order to be completely explicit about the gauge indices. Recalling the form of the Lorentz generators for the vector representation,

$$(\mathcal{J}^{\rho\sigma})_{\alpha\beta} = i\left(\delta^\rho_\alpha \delta^\sigma_\beta - \delta^\sigma_\alpha \delta^\rho_\beta\right), \tag{3.55}$$

we see that this object has the same formal structure as the fermion action,

$$\mathcal{L}_{\text{gauge}} = -\frac{1}{2g^2}\left\{a^a_\mu \left[(-D^2)^{ac} g^{\mu\nu} + 2\left(\frac{1}{2}\mathcal{F}^b_{\rho\sigma}\mathcal{J}^{\rho\sigma}\right)^{\mu\nu} \left(t^b_G\right)^{ac}\right] a^c_\nu\right\}. \tag{3.56}$$

[1] The details of these computations are outlined in the exercises. Here we are following closely the presentation in the text by Peskin and Schroeder (1995).

https://doi.org/10.1017/9781009290883.008 Published online by Cambridge University Press

Finally, the Faddeev–Popov Lagrangian is just

$$\mathcal{L}_c = \bar{c}^a[-(D^2)^{ab}]c^b. \tag{3.57}$$

Since the ghost fields are Lorentz scalars, this Lagrangian has the same form as the others. We need, then, to evaluate a product of determinants of the form

$$\det\left[-D^2 + 2\left(\frac{1}{2}\mathcal{F}^b_{\rho\sigma}\mathcal{J}^{\rho\sigma}\right)t^b\right] \tag{3.58}$$

with t and $\mathcal{J}$ the generators appropriate to the representation.

The term in parentheses can be written as

$$\Delta_{r,j} = -\partial^2 + \Delta^{(1)} + \Delta^{(2)} + \Delta^{(\mathcal{J})} \tag{3.59}$$

with

$$\begin{aligned}\Delta^{(1)} &= i\left(\partial^\mu A^a_\mu t^a + \mathcal{A}^a_\mu t^a \partial^\mu\right)\\ \Delta^{(2)} &= \mathcal{A}^{a\mu} t^a \mathcal{A}^b_\mu t^b.\\ \Delta^{(\mathcal{J})} &= 2\left(\frac{1}{2}\mathcal{F}^b_{\rho\sigma}\mathcal{J}^{\rho\sigma}\right)t^b.\end{aligned} \tag{3.60}$$

The action we are seeking is the log of the determinant. We are interested in this action expanded to second order in $\mathcal{A}$ and second order in ∂^2:

$$\begin{aligned}\ln\det(\Delta_{r,j}) = \ln\det(-\partial^2) + \mathrm{tr}\Big[&(-\partial^2)^{-1}\left(\Delta^{(1)} + \Delta^{(2)} + \Delta^{(\mathcal{J})}\right)\\ &- \frac{1}{2}\left((-\partial^2)^{-1}\Delta^{(1)}(-\partial^2)^{-1}\Delta^{(1)}\right)\Big],\end{aligned} \tag{3.61}$$

where $1/(-\partial^2)$ is the propagator for a scalar field. So this has the structure of a set of one-loop diagrams in a scalar field theory. Since we are working to quadratic order, we can take the $\mathcal{A}$ field to carry momentum k. The term involving two factors $\Delta^{(1)}$ is in some ways the most complicated to evaluate. Note that the trace is a trace in coordinate space and over the gauge and Lorentz indices. In momentum space the space–time trace is just an integral over momenta. We take all the momenta to be Euclidean. So the result is given, in momentum space, by

$$\frac{1}{2}\int\frac{d^dk}{(2\pi)^d}\mathcal{A}^a_\mu(k)\mathcal{A}^b_\nu(-k)\int\frac{d^dp}{(2\pi)^d}\,\mathrm{Tr}\left[\frac{1}{p^2}(2p+k)^\mu t^a\frac{1}{(p+k)^2}(2p+k)^\nu t^b\right]. \tag{3.62}$$

This has precisely the structure of one of the vacuum polarization diagrams of scalar electrodynamics (see Fig. 3.7). The other contribution arises from the factor $\Delta^{(2)}$. Combining the two contributions, and performing the integral by dimensional regularization gives

$$\frac{1}{2}\int\frac{d^dk}{(2\pi)^d}\mathcal{A}^a_\mu(-k)\mathcal{A}^b_\nu(k)(k^2g^{\mu\nu} - k^\mu k^\nu)\left[\frac{C(r)d(j)}{3(4\pi)^2}\Gamma\left(2-\frac{d}{2}\right)(k^2)^{2-d/2}\right], \tag{3.63}$$

https://doi.org/10.1017/9781009290883.008 Published online by Cambridge University Press

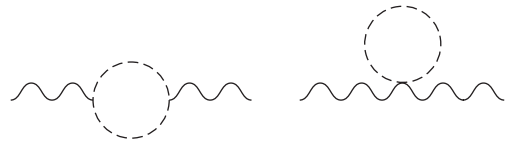

Fig. 3.7 The background-field calculation has the structure of scalar electrodynamics.

where $C(r)$ is a Casimir operator, encountered previously. The quantities $C(j)$ are similar quantities for the Lorentz group: $C(j) = 0$ for scalars, 1 for Dirac spinors and 2 for four-vectors. To quadratic order in the external fields, the transverse terms above give $(\mathcal{F}^{\mu\nu})^2$.

The contribution involving $\Delta^{(\mathcal{J})}$ in Eq. (3.61) is even simpler to evaluate, since the needed factors of momentum (which are derivatives) are already included in $\mathcal{F}$. The rest is bookkeeping; the required action has the form

$$\mathcal{L}_{\text{eff}} = -\frac{1}{4}\left[\frac{1}{g^2} + \frac{1}{2}\left(C_G - C_c - \frac{n_f}{2}C_{n_f}\right)\right]F_{\mu\nu}^2 \tag{3.64}$$

where

$$C_i = c_i \frac{1}{16\pi^2}\left(\frac{2}{\epsilon} - \ln k^2\right), \quad c_G = -\frac{20}{3}, \quad c_c = 3, \quad c_{n_f} = -\frac{1}{3}. \tag{3.65}$$

This gives precisely Eq. (3.21).

3.7 The strong interactions and dimensional transmutation

In QCD the only parameters at the classical level with the dimensions of mass are the quark masses. In a world with just two light quarks, u and d, we would not expect the properties of hadrons to be very different from the observed properties of the non-strange hadrons. However, the masses of the up and down quarks are quite small; in fact, as we will see, too small to account for the masses of the non-strange hadrons such as the proton and neutron. In other words, in the limit of zero quark mass these hadrons would not become massless. How can a mass arise in a theory with no classical mass parameters?

While classically QCD is scale invariant, this is not true quantum mechanically. We have seen that we must specify the value of the gauge coupling at a particular energy scale; in the language we have used up to now, the theory is specified by giving the Lagrangian associated with a particular cutoff scale. If we change this scale, we have to change the values of the parameters, and physical quantities such as the proton mass $m_p = u$, should be unaffected. Using our experience with the renormalization group we can write down a differential equation which expresses how such a mass depends on g and μ, so that the mass is independent of which scale we choose to define our theory:

$$\left[\mu\frac{\partial}{\partial\mu} + \beta(g)\frac{\partial}{\partial g}\right]m_p = 0. \tag{3.66}$$

https://doi.org/10.1017/9781009290883.008 Published online by Cambridge University Press

We know the solution of this equation:

$$m_p = C\mu \exp\left[-\int \frac{dg'}{\beta(g')}\right]. \tag{3.67}$$

To lowest order in the coupling,

$$m_p = C\mu \exp\left[-\frac{8\pi^2}{g^2(\mu)}\right]. \tag{3.68}$$

This phenomenon, that a physical mass scale can appear as a result of the need to introduce a cutoff in the quantum theory, is called *dimensional transmutation*. In the next section we will discuss this phenomenon as it occurs in lattice gauge theory. Later we will describe a two-dimensional model with which we can do a simple computation that exhibits the dynamical appearance of a mass scale.

3.8 Confinement and lattice gauge theory

The fact that QCD becomes weakly coupled at high momentum transfers has allowed rigorous comparison with experiment. Despite the fact that the variation of the coupling is only logarithmic, experiments are sufficiently sensitive, and have covered a sufficiently broad range of q^2, that such comparisons are possible. Still, many of the most interesting questions of hadronic physics – and some of the most interesting challenges of quantum field theory – are problems of low momentum transfer. Here one encounters the flip side of asymptotic freedom: at large distances, the theory is necessarily strongly coupled and perturbative methods are not useful. It is, perhaps, frustrating that we cannot compute the masses of the low-lying hadrons in a fashion analogous to the calculation of the properties of simple atoms. Perhaps even more disturbing is that we cannot give a simple argument that quarks are confined or that QCD exhibits a mass gap. To deal with these questions, we will first ask a somewhat naive question: what can we say about the path integral, or for that matter the Hamiltonian, in the limit in which the coupling constant becomes very large? This question is naive in that the coupling constant is not really a parameter of this theory. It is a function of the scale, and the important scale for binding hadrons is that where the coupling becomes of order one. Let us consider the problem anyway. We will start with a pure gauge theory, i.e. a theory without fermions or scalars. Consider, first, the path integral. To extract the spectrum, it should be adequate to consider the Euclidean version:

$$Z = \int [dA_\mu] \exp\left(-\frac{1}{4g^2} F_{\mu\nu}^2\right). \tag{3.69}$$

Let us contrast the weak- and strong-coupling limits of this expression. At weak coupling $1/g^2$ is large, so fluctuations are highly damped; we might expect the action to be controlled by the stationary points. The simplest such stationary point occurs where $F_{\mu\nu} = 0$, and this is the basis of perturbation theory. Later we will see that there are other interesting stationary points – classical solutions of the Euclidean equations.

https://doi.org/10.1017/9781009290883.008 Published online by Cambridge University Press

Now consider strong coupling. As $g \to \infty$ the action vanishes – there is no damping of the quantum fluctuations. It is not obvious how one can develop any sort of approximation scheme. We can consider this problem, alternatively, from a Hamiltonian point of view. A convenient gauge for this purpose is the gauge $A_0 = 0$. In this gauge Gauss's law is a constraint that must be imposed on states. As we will discuss shortly, Gauss's law is (almost) equivalent to the condition that the quantum states must be invariant under time-independent gauge transformations. In the $A^0 = 0$ gauge, the canonical momenta are very simple:

$$\Pi^i = \frac{\partial \mathcal{L}}{\partial \dot{A}^i} = -\frac{1}{g^2} E^i. \tag{3.70}$$

So, the Hamiltonian is

$$\mathcal{H} = \frac{g^2}{2} \vec{\Pi}^2 + \frac{1}{2} \vec{B}^2. \tag{3.71}$$

In the limit $g^2 \to \infty$, the magnetic terms are unimportant and the Π^2 terms dominate. So we should somehow work, in lowest order, with states which are eigenstates of $\vec{E}$. In any approach which respects even rotational covariance, it is unclear how to proceed.

The solution to both dilemmas is to replace the space–time continuum with a discrete lattice of points. In the Lagrangian approach one introduces a space–time lattice. In the Hamiltonian approach one keeps the time continuous but makes space discrete. Clearly there is a large price for such a move: one gives up Lorentz invariance, even rotational invariance. At best, Lorentz invariance is something which one can hope to recover in the limit where the lattice spacing is small compared with the relevant physical distances. There are several rewards, however.

1. One has a complete definition of the theory which does not rely on perturbation theory.
2. The lattice, at strong coupling, gives a simple model of confinement.
3. One obtains a precise procedure in which to calculate the properties of hadrons. With large enough computing power one can in principle calculate the properties of low-lying hadrons with arbitrary precision.

There are other difficulties which must be overcome. Not only is rotational symmetry lost, but other approximate symmetries – particularly chiral symmetries – are complicated. But, over time, combining ingenuity and growing computer power there has been enormous progress in numerical lattice computations. Lattice gauge theory has developed into a highly specialized field of its own, and we will not do justice to it here. However, given the importance of field theories – often strongly coupled field theories – not only for our understanding of QCD but for any understanding of physics beyond the Standard Model, it is worthwhile to briefly introduce the subject here.

3.8.1 Wilson's formulation of lattice gauge theory

In introducing a lattice the hope is that, as one allows the lattice spacing a to become small, one will recover Lorentz invariance. A little thought is required to understand what

https://doi.org/10.1017/9781009290883.008 Published online by Cambridge University Press

is meant by *small*. The only scale in the problem is the lattice spacing. But there is another important parameter: the gauge coupling. The value of this coupling, we might expect, should be thought of as the QCD coupling at scale a. So, taking small lattice spacing means physically taking the gauge coupling to be weak. At small lattice spacing, the short-distance Green's functions will be well approximated by their perturbative expansions. On the other hand, the smaller the lattice, the more numerical power required to compute the physically interesting, long-distance, quantities.

There is one symmetry which one might hope to preserve as one introduces a space–time lattice: gauge invariance. Without it, there are many sorts of operators which could appear in the continuum limit and recovering the theory of interest would be likely to be very complicated. Wilson pointed out that there is a natural set of variables to work with; there are known as *Wilson lines*. Consider, first, a $U(1)$ gauge theory. Under a gauge transformation $A_\mu(x) \to A_\mu + ig(x)\partial_\mu g^\dagger(x)$, where $g(x) = e^{i\alpha(x)}$, the object

$$U(x_1, x_2) = \exp\left(i \int_{x_1}^{x_2} dx_\mu A^\mu\right),$$

transforms as follows:

$$U(x_1, x_2) \to g(x_1) U(x_1, x_2) g^\dagger(x_2). \tag{3.72}$$

So, for example, for a charged fermion field $\psi(x)$ transforming as $\psi(x) \to g(x)\psi(x)$, a gauge-invariant operator is

$$\psi^\dagger(x_1) U(x_1, x_2) \psi(x_2). \tag{3.73}$$

From gauge fields alone one can construct an even simpler gauge-invariant object, a Wilson line beginning and ending at some point x:

$$U(x, x) = \exp\left(i \oint_C dx^\mu A_\mu\right), \tag{3.74}$$

where U is called a Wilson loop.

These objects have a simple generalization in non-Abelian gauge theories. Using the matrix form for A_μ the main issue is one of ordering. The required ordering prescription is a path ordering, P:

$$U(x_1, x_2) = P \exp\left(i \int_{x_1}^{x_2} dx^\mu A_\mu\right). \tag{3.75}$$

It is not hard to show that the transformation law for the Abelian case generalizes to the non-Abelian case:

$$U(x_1, x_2) \to g(x_1) U(x_1, x_2) g^{-1}(x_2). \tag{3.76}$$

To see this, note first that path ordering is like time ordering so, if s is the parameter of the path, U satisfies

$$\frac{d}{ds} U(x_1(s), x_2) = \left(ig \frac{dx^\mu}{ds} A_\mu(x_1(s))\right) U(x_1(s), x_2) \tag{3.77}$$

https://doi.org/10.1017/9781009290883.008 Published online by Cambridge University Press

or, more elegantly,

$$\frac{dx_1^\mu}{ds} D_\mu U(x_1, x_2) = 0. \tag{3.78}$$

Now suppose that $U(x_1, x_2)$ satisfies the transformation law (Eq. (3.72)). Then it is straightforward to check, from Eq. (3.77), that $U(x_1 + dx_1, x_2)$ satisfies the correct equation. Since U satisfies a first-order differential equation, this is enough.

Again, the integral around a closed loop, C, is gauge invariant, provided that now one takes the trace:

$$U(x_1, x_1) = \mathrm{Tr}\, \exp\left(i \oint_C dx^\mu A_\mu \right). \tag{3.79}$$

Wilson used these objects to construct a discretized version of the usual path integral. Take the lattice to be a simple hypercube, with points $x^\mu = an^\mu$, where n^μ is a vector of integers and a is called the lattice spacing. At any point x one can construct a simple Wilson line $U(x)_{\mu\nu}$, known as a *plaquette*. This is just the product of Wilson lines around a unit square. Letting n_μ denote a unit vector in the μ direction, we denote the Wilson line $U(x, x + an^\mu)$ by $U(x)_\mu$. These are the basic variables; as they are associated with the lines linking two lattice points they are called *link variables.* Then the Wilson loops about each plaquette are denoted as follows:

$$U(x)_{\mu\nu} = U(x)_\mu U(x + an^\mu)_\nu U(x + an^\mu + an^\nu)_{-\mu} U(x + an^\nu)_{-\nu}. \tag{3.80}$$

In the non-Abelian case, a trace is understood to be taken. For small a, in the Abelian case it is easy to expand $U_{\mu\nu}$ in powers of a and to show that

$$U(x)_{\mu\nu} \approx \exp\left[ia^2 F_{\mu\nu}(x)\right]. \tag{3.81}$$

So, we can write down an action which in the limit of small lattice spacing goes over to the Yang–Mills action:

$$S_{\mathrm{Wilson}} = \frac{1}{4g^2} \sum_{x,\mu,\nu} U(x)_{\mu,\nu}. \tag{3.82}$$

In the non-Abelian case this same expression holds, except with the factor 4 replaced by 2 and a trace over the U matrices.

How might we investigate the question of confinement with this action? Here, Wilson also made a proposal. Consider the amplitude for a process in which a very heavy (infinitely heavy) quark–antiquark pair, separated by a distance R, was produced in the far past and allowed to propagate for a long time T after which the pair annihilates. In Minkowski space the amplitude for this would be given by

$$\langle f | e^{-iHT} | i \rangle, \tag{3.83}$$

where H is the Hamiltonian for the process. If we transform to Euclidean space and insert a complete set of states, for each state we have a factor $\exp(-E_n T)$. As $T \to \infty$ this becomes $e^{-E_0 T}$, where E_0 is the ground state of the system with two infinitely massive quarks separated by a distance R, and is what we would naturally identify with the potential of the quark–antiquark system.

https://doi.org/10.1017/9781009290883.008 Published online by Cambridge University Press

In the path integral this expectation value is precisely the Wilson loop U_P, where P is the path from the point of production to the point of annihilation and back. If the quarks only experience a Coulomb force, one expects the Wilson loop to behave as

$$\langle U_P \rangle \propto e^{-\alpha T/R} \tag{3.84}$$

for a constant α. In other words, the exponential behaves as the *perimeter* of the loop. If the quarks are confined, with a linear confining force, the exponential behaves as e^{-bTR}, i.e. as the *area* of the loop. So Wilson proposed to measure the expectation value of the Wilson loop and determine whether it obeyed a perimeter or area law.

In strong coupling it is a simple matter to do the computation in the lattice gauge theory. We are interested in

$$\int \prod dU(x)_\mu \, \exp\left(-S_{\text{lattice}} + i \prod_{\text{P}} U\right). \tag{3.85}$$

We can evaluate this by expanding the exponent in powers of $1/g^2$. Because

$$\int dU_\mu \, U_\mu = 0, \quad \int dU_\mu \, U_\mu U_\mu^\dagger = \text{const} \tag{3.86}$$

(you can check this easily in the Abelian case), in order to obtain a non-vanishing result we need to tile the path with plaquettes, as indicated in Fig. 3.8. So the result is exponential in the area,

$$\langle U_P \rangle = \left(\frac{\text{const}}{g^2}\right)^A, \tag{3.87}$$

and the force law is

$$V(R) = \text{const} \times \frac{g^2}{a^2} R. \tag{3.88}$$

This is not a proof of confinement in QCD. First note that this result holds in the strong coupling limit of either an Abelian or a non-Abelian gauge theory. This is possible because

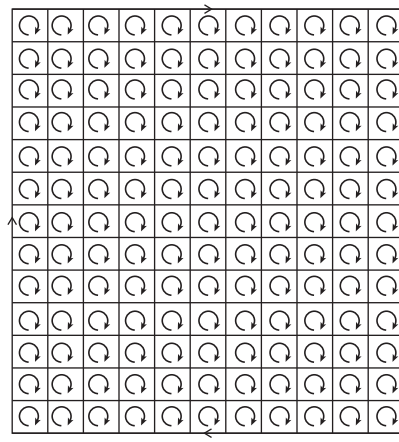

Fig. 3.8 Leading non-vanishing contribution to the Wilson loop in strong coupling lattice gauge theory.

https://doi.org/10.1017/9781009290883.008 Published online by Cambridge University Press

even the pure gauge Abelian lattice theory is an interacting theory. From this we learn that the strong coupling behavior of a lattice theory can be very different than the weak coupling behavior. For QCD we would like to choose the lattice spacing to correspond to a small physical scale, say $a = (4\ \text{GeV})^{-1}$, where the gauge coupling is small, and then study the behavior of the correlation functions, Wilson loops and other quantities on much larger scales. At present this requires numerical techniques.

3.8.2 Hamiltonian lattice gauge theory

Before discussing Hamiltonian lattice gauge theories, it is interesting to see how the strong-coupling result arises from a Hamiltonian viewpoint. To simplify the computation we consider a $U(1)$ gauge theory. In the Hamiltonian approach the basic dynamical variables are the matrices U_i associated with the spatial directions. There is also the gauge field A_0. As in continuum field theory, we can choose $A_0 = 0$. In this gauge, in the continuum the dynamical variables are A_i and their conjugate momenta are E_i; on the lattice, the momenta conjugate to the U_i are the E_i. The Hamiltonian has the form

$$H = \sum \frac{g^2 \vec{\Pi}(x)^2}{a} + \frac{1}{4g^2} \sum U_{ij}(\vec{x}) \frac{1}{a}. \tag{3.89}$$

The U_is are compact variables, so the $\Pi(x)$s at each point are like angular momenta. At strong coupling this is a system of decoupled rotors. The ground state of the system has a vanishing value of these angular momenta.

Now introduce a heavy quark–antiquark pair to the system, separated by a distance R in the z direction. In the $A_0 = 0$ gauge, states must be gauge invariant (we will discuss this further when we consider instantons, in the next chapter). So, a candidate state has the form

$$|\Psi\rangle = q^\dagger(0) U_z(0, R) \bar{q}^\dagger(R) |0\rangle. \tag{3.90}$$

Here

$$U_z(0, R) = U_z(0, 1) U_z(1, 2) \cdots U_z(N-1, N), \tag{3.91}$$

where $R = Na$. Now we can evaluate the expectation value of the Hamiltonian in this state. At strong coupling we can ignore the magnetic terms. The effect of the U_z operators is to raise the "angular momentum" associated with each link by one unit (in the $U(1)$ case, $U_z(n, n+1) = e^{i\theta_{n+1}}$). So the energy of the state is just

$$a^{-1} g^2 N, \tag{3.92}$$

and the potential grows linearly with separation.

3.8.3 Numerical methods in lattice gauge theory; introduction of fermions

We have seen that the strong coupling analysis, while providing a model for confinement, is hardly satisfactory. It predicts confinement in lattice QED as well as QCD. It turns out that in QED there is a phase transition (a discontinuous change of behavior) between the

https://doi.org/10.1017/9781009290883.008 Published online by Cambridge University Press

strong- and weak-coupling phases. To be sure that the same does not occur in QCD, we need to evaluate the Wilson line on a very fine lattice, at large separation. This means we need to work with an action having a *small* coupling. To put it another way, to reliably describe, say, a proton we need to use a lattice on which the spacing a is much smaller than the QCD scale. At present such studies can only be undertaken by evaluating the lattice path integral numerically. In principle, since the lattice theory reduces space–time to a finite number of points, the required path integral is just an ordinary integral, albeit with a huge number of dimensions. For example, if we have a $10 \times 10 \times 10 \times 10$ lattice, with of order 10^4 links (each a 3×3 matrix), and quarks at each site, it is clear that a straightforward numerical evaluation involves an exponentially large number of operations. In practice it is necessary to use Monte Carlo (statistical sampling) methods to evaluate the integrals. These techniques are now sufficiently powerful to demonstrate convincingly an area law at weak coupling. The constant in the area law, the coefficient of the linear term in the quark–antiquark potential, is a dimensionful parameter. It must be renormalization-group invariant. As a result, it must take the form

$$T = ca^{-2} \exp\left[-\int \frac{dg'}{\beta(g')}\right]. \tag{3.93}$$

At weak coupling we know the form of the beta function, so we know how T should behave as we vary the lattice spacing and coupling. The results of numerical studies are in good agreement with these expressions.

However, we would like to study real QCD, with fermions. Fermions introduce additional challenges. These are of two types. First, one needs a strategy to deal with Grassman integrations in the functional integral. The usual strategy is to hold the bosonic variables fixed while first performing the integral over the fermions. This yields a determinant (in general multiplied by some Green's functions), which must be evaluated for every value of the bosonic integrand. These are determinants of enormous matrices and must themselves be evaluated by statistical techniques. In the early years of lattice gauge theory, such computations were out of reach and so numerical work generally simply dropped the determinant (such calculations were said to be *quenched*). But, by the early years of the new millennium, both algorithms for these computations and computer power had developed to the point that such computations were feasible.

As we will see further in Chapter 5, it is crucial to our understanding of the strong interactions that the u, d and s quarks are light compared with the characteristic scales of the strong interactions and in particular compared with quantities such as the pion decay constant and the ρ meson mass. However, massless or light fermions, on the lattice, are problematic. The difficulties are associated with the fact that their kinetic terms are first order in derivatives. Writing the derivative as a naive difference leads to the problem of fermion "doubling".

To see the difficultly, consider first the kinetic terms for a free boson. Label the lattice points (in a Euclidean lattice) by four vectors $n_\mu a$, where a is the lattice spacing, i.e. $x_\nu = n_\nu a$. Then

$$\partial_\mu \phi(x) \to [\phi(x + n_\mu a) - \phi(x - n_\nu a)]/(2a). \tag{3.94}$$

https://doi.org/10.1017/9781009290883.008 Published online by Cambridge University Press

Now we write a Fourier expansion in terms of

$$\phi_k e^{ik_\mu x_\mu}, \tag{3.95}$$

where $-\pi/a \leq k^\mu \leq \pi/a$. This is the analog of the familiar problem of a particle in a box of size L with periodic boundary conditions. There $k = 2\pi n/L$. Now the roles of x and k are reversed: $x = na$, so k lies in an interval of size $2\pi/a$, as above. Then, for scalars, the second derivative term, defined as above, is proportional to

$$|f_k|^2(1 - \cos\, k_\mu a) \tag{3.96}$$

which is consistent with the size of the k interval.

However, for fermions, a term such as $\partial_\mu \gamma_\mu$ is proportional to

$$f_k \gamma_\mu \sin\, k_\mu a \tag{3.97}$$

which has zeros (corresponding to poles in the propagator) not only at $k_\mu = 0$ but also at points where the components $k_\mu = \pi/a$. The appearance of these extra light degrees of freedom is called the *fermion doubling problem*. General theorems show that it is unavoidable. In practice this problem is dealt with in either of two ways. One can attempt to treat the extra fermions as additional light flavors, or one can add a term to the action which gives mass to the extra fermions, typically a term proportional to a parameter and $1 - \cos\, ka$, known as the Wilson term. The price of the first method is that one must extract results for the actual number of flavors (three) from a theory with more flavors. This has been the approach of the MILC collaboration, one of the large lattice simulation efforts. In the second method one has the difficulty that the parameters must be tuned, as one approaches the continuum limit, in such a way that one obtains the expected symmetry structure of actual QCD. This method has been used by the BMW collaboration and others. Considerable success has been achieved with both, and there is remarkable agreement. A third method is known as the *domain wall fermion* method. Here one introduces a fifth dimension, with fields of opposite chirality living on two walls. This method shows promise but imposes additional computational challenges and to date has been numerically less extensively studied.

3.9 Strong interaction processes at high momentum transfer

Quantum chromodynamics has been tested with high precision in a variety of processes at high momentum transfer (short distances). It is by now an important tool in probing for new physics in particle colliders. Indeed, our understanding of perturbative QCD was crucial to the discovery of the Higgs boson. It is these processes to which one can apply ordinary perturbation theory. If Q^2 is the typical momentum transfer of a process, cross sections are given by a power series in $\alpha_s(Q^2)$. The application of perturbation theory, however, is subtle. In accelerators we observe hadrons; using perturbation theory we compute the production rate for quarks and gluons. We will briefly survey some applications in this section. The simplest process to analyze is e^+e^- annihilation, and we discuss it first.

https://doi.org/10.1017/9781009290883.008 Published online by Cambridge University Press

Then we turn to processes involving the deep inelastic scattering of leptons by hadrons and follow this by considering by processes involving hadrons only. Finally, we describe recent progress in QCD computations for processes involving complicated final states (many gluons) and/or higher orders in perturbation theory.

3.9.1 e^+e^- annihilation

At the level of quarks and gluons, the first few diagrams contributing to the production cross section are exhibited in Fig. 3.9. There is, in perturbation theory, a variety of final states, $q\bar{q}$, $q\bar{q}g$, $q\bar{q}gg$, $q\bar{q}q\bar{q}$ and so on. We do not understand, in any detail, how these quarks and gluons materialize as the observed hadrons. But we might imagine that this occurs as in Fig. 3.10. The initial quarks radiate gluons which can in turn radiate quark–antiquark pairs. As the cascade develops, quarks and antiquarks can pair to form mesons, qqq combinations can form baryons and so on. In these complex processes (called *hadronization*) we can construct many relativistic invariants and many of these will be small, so that perturbation theory cannot be trusted. In a sense this is good; otherwise, we would be able to show that free quarks and gluons were produced in the final states. But if we only ask about the *total* cross section, each term in the series is a function only of the center of mass energy s. As

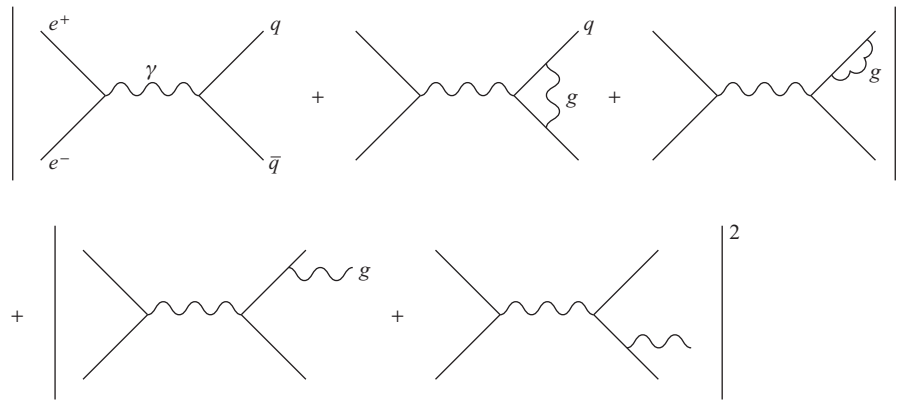

Fig. 3.9 Low-order contributions to e^+e^- annihilation.

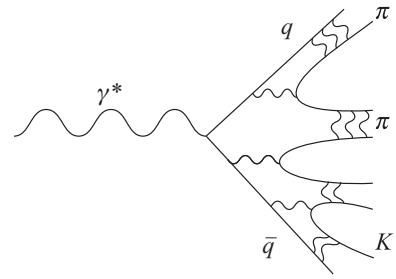

Fig. 3.10 Emission of gluons and quarks leads to the formation of hadrons.

https://doi.org/10.1017/9781009290883.008 Published online by Cambridge University Press

a result, if we simply choose s for the renormalization scale, the cross section is given by a power series in $\alpha_s(s)$. One way to see this is to note that the cross section is proportional to the imaginary part of the photon vacuum polarization tensor, $\sigma(s) \propto \text{Im}\ \Pi$. One can calculate Π in Euclidean space and then analytically continue. In the Euclidean calculation there are no infrared divergences, so the only scales are s and the cutoff (or renormalization scale). It is convenient to consider the ratio

$$R(e^+e^- \to \text{ hadrons}) = \frac{\sigma(e^+e^- \to \text{ hadrons})}{\sigma(e^+e^- \to \mu^+\mu^-)}. \tag{3.98}$$

The lowest-order (α_s^0) contribution can be written down without any work:

$$R(e^+e^- \to \text{ hadrons}) = 3\sum Q_f^2, \tag{3.99}$$

where we have explicitly pulled out a factor 3 for color and the sum is over those quark flavors light enough to be produced at energy $\sqrt{s}$. So, for example, above the charm quark threshold and below the bottom quark threshold this would give

$$R(e^+e^- \to \text{ hadrons}) = \frac{10}{3}. \tag{3.100}$$

Before comparing with the data we should consider corrections. The cross section has been calculated through order α_s^3, where $\alpha_s = g_s^2/(4\pi)$; g_s, the strong coupling constant was introduced in Eq. (2.64). Here we quote just the first two orders:

$$R(e^+e^- \to \text{ hadrons}) = 3\sum Q_f^2\left(1 + \frac{\alpha_s}{\pi}\right). \tag{3.101}$$

This may be compared with the data in Fig. 3.11.

This calculation has other applications. Among these are applications to the widths of the Z and of the τ lepton. The decays of Z_s to hadrons involve essentially the same Feynman diagrams as before (Fig. 3.12), except for the different Z couplings to the quarks. This may be compared with experiment using Table 3.1.

3.9.2 Jets in e^+e^- annihilation

Much more is measured in e^+e^- annihilation than the total cross section, and clearly we would like to extract further predictions from QCD. If we are to use perturbation theory then it is important that we limit our questions to processes for which all momentum transfers are large. It is also important that perturbation theory should *fail* for some questions. After all, we know that the final states observed in accelerators contain hadrons, not quarks and gluons. If perturbation theory were good for sufficiently precise descriptions of the final state, the theory would simply be wrong.

To understand the issues, let us briefly recall some features of QED for a process like $e^+e^- \to \mu^+\mu^-$. At lowest order one just has the production of a $\mu^+\mu^-$ pair. At order α, however, one has final states with an additional photon and loop corrections to the muon lines (also to the electron or positron lines), as indicated in Fig. 3.13. Both the loop corrections and the total cross section for final states with a photon are infrared divergent. In QED the answer to this problem is *resolution*. In an experiment one cannot detect a photon

https://doi.org/10.1017/9781009290883.008 Published online by Cambridge University Press

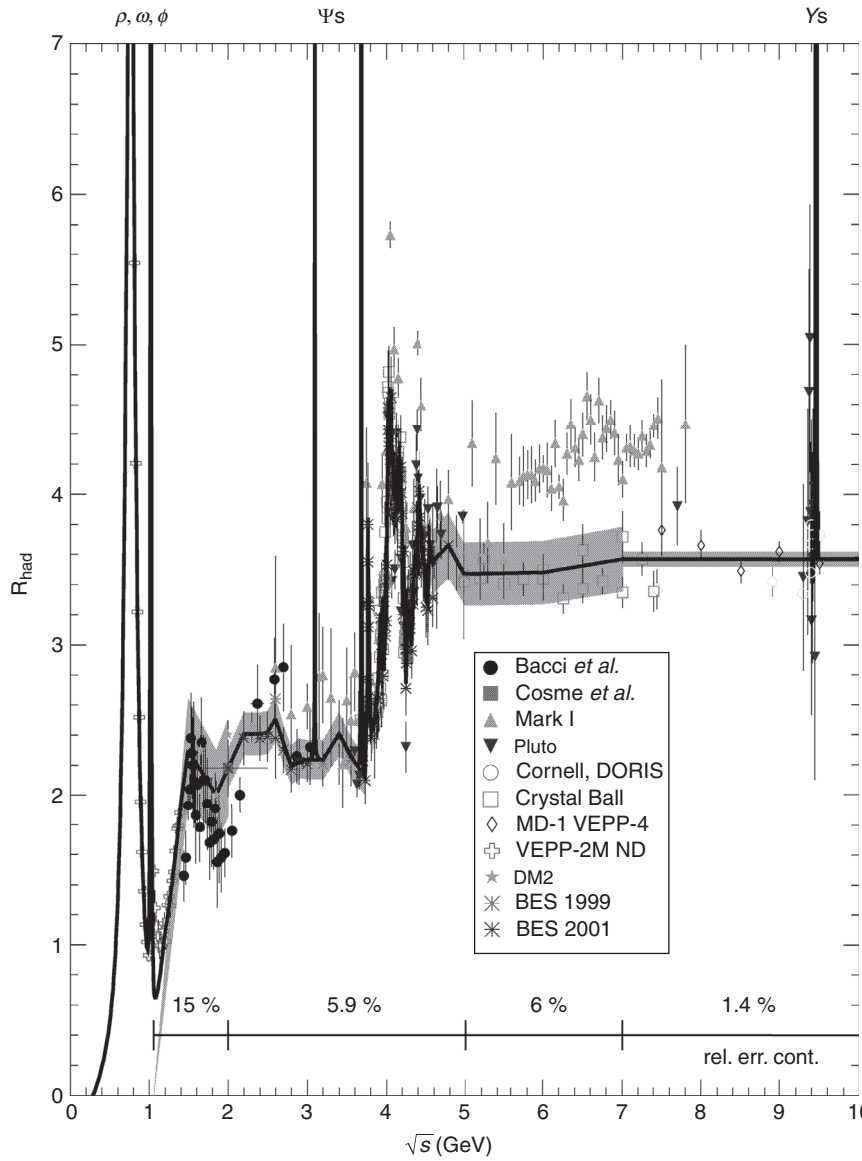

Fig. 3.11 Experimental data for the ratio R in e^+e^- annihilation, together with the theoretical prediction from Eq. (3.101). Reproduced from H. Burkhardt and B. Pietrzyk, *Phys. Lett. B* **513**, 46 (2001). Copyright 2001, with permission from Elsevier.

of arbitrarily low energy. So, in comparing the theory with the observed cross section for $\mu^+\mu^-$ (with no photon), one must allow for the possibility that a very-low-momentum photon is emitted and not detected. By including some energy resolution ΔE the cross sections for each possible final state are made finite. If the energy is very large one also has to keep in mind that experimental detectors cannot resolve photons that are nearly

https://doi.org/10.1017/9781009290883.008 Published online by Cambridge University Press

Table 3.1 Experimental and theoretical values of properties of the Z boson. Note the close agreement at the one part in 10^2—10^3 level. Reprinted from *Electroweak Model and Constraints on New Physics*, Particle Data Group (2005), and S. Eidelman *et al.*, *Phys. Lett. B*, **592**, 1 (2004) (used with permission of the Particle Data Group and Elsevier)

Quantity	Value	Standard Model	Pull
m_t (GeV)	176.1 ± 7.4	176.96 ± 4.0	-0.1
	180.1 ± 5.4		0.6
M_W (GeV)	80.454 ± 0.059	80.390 ± 0.018	1.1
	80.412 ± 0.042		0.5
M_Z (GeV)	91.1876 ± 0.0021	91.1874 ± 0.0021	0.1
Γ_Z (GeV)	2.4952 ± 0.0023	2.4972 ± 0.0012	-0.9
Γ(had) (GeV)	1.7444 ± 0.0020	1.7435 ± 0.0011	—
Γ (inv) (MeV)	499.0 ± 1.5	501.81 ± 0.13	—
$\Gamma(\ell^+\ell^-)$ (MeV)	83.984 ± 0.086	84.024 ± 0.025	—
σ_{had} (nb)	41.341 ± 0.037	41.472 ± 0.000	1.9

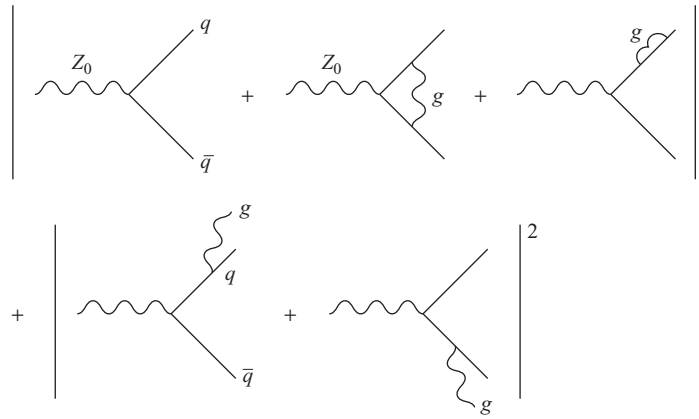

Fig. 3.12 Feynman diagrams contributing to Z decay are similar to those in e^+e^- annihilation.

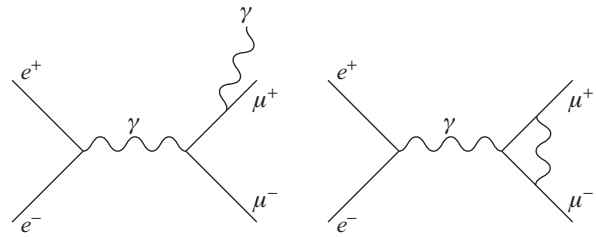

Fig. 3.13 The infrared problem.

https://doi.org/10.1017/9781009290883.008 Published online by Cambridge University Press

parallel to one or other of the outgoing muons. The cross section, again, for each type of final state has large logarithms, $\ln(E/m_\mu)$. These are often called *collinear singularities* or *mass singularities.* So one must allow for the finite angular resolution of real experiments. Roughly speaking, then, the radiative corrections for these processes involve

$$\delta\sigma \propto \frac{\alpha}{4\pi} \ln \frac{E}{\Delta E} \ln \Delta\theta. \tag{3.102}$$

As one makes the energy resolution, or the angular resolution smaller, perturbation theory becomes poorer. In QED it is possible to sum these large double-logarithmic terms.

In QCD these same issues arise. Partial cross sections are infrared divergent. One obtains finite results if one includes an energy and angular resolution. But now the coupling is not as small as in QED, and it grows with energy. In other words, if one takes an energy resolution much smaller than the typical energy in the process, or an angular resolution which is very small, the logarithms which appear in the perturbation expansion signal that the expansion parameter is not $\alpha_s(s)$ but something more like $\alpha_s(\Delta E)$ or $\alpha_s(\Delta\theta s)$. So perturbation theory eventually breaks down.

However, if one does not make ΔE or $\Delta\theta$ too small then perturbation theory should be valid. Consider, again, e^+e^- annihilation to hadrons. One might imagine that on the one hand the processes which lead to the observed final states would involve the emission of many gluon and quark–antiquark pairs from the initial outgoing $q\bar{q}$ pair, as in Fig. 3.10. The final emissions will involve energies and momentum transfers of order the masses of pions and other light hadrons, and perturbation theory will not be useful. On the other hand, we can restrict our attention to the kinematic regime where the gluon is emitted at a large angle relative to the quark and has a substantial energy. There are no large logarithms in this computation, nor in the computation of the $q\bar{q}$ final state. We can give a similar definition for the $q\bar{q}g$ final state. From an experimental point of view, this means that we expect to see jets of particles (or of energy–momentum) that are reasonably collimated, and that we should be able to calculate the cross sections for the emission of such jets. These calculations are similar to those of QED. Such jets are observed in e^+e^- annihilation, and their angular distribution agrees well with theoretical prediction. When first observed, these three-jet events were described, appropriately, as the discovery of the gluon.

3.9.3 Deep inelastic scattering

Deep inelastic scattering was one of the first processes to be studied theoretically in QCD. These are experiments in which a lepton is scattered at high momentum transfer from a nucleus. The lepton can be an electron, a muon or a neutrino; the exchanged particle can be a γ, $W^\pm$ or Z (Fig. 3.14). One does not ask about the details of the final hadronic state but simply how many leptons are scattered at a given angle. Conceptually, these experiments are like Rutherford's experiment which discovered the atomic nucleus. In much the same way, they showed that nucleons contain quarks, having just the charges predicted by the quark model.

In the early days of QCD this process was attractive to study theoretically, because one can analyze it without worrying about issues about defining jets and the like. The inclusive

https://doi.org/10.1017/9781009290883.008 Published online by Cambridge University Press

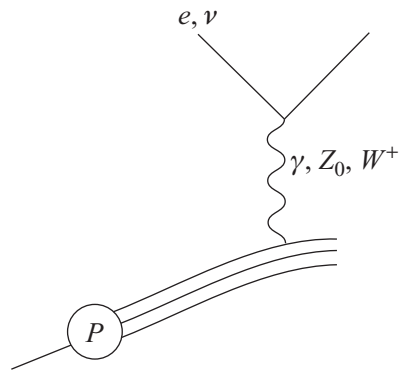

Fig. 3.14 The deep inelastic scattering of leptons from a nucleon.

cross section can be related, by unitarity, to a correlation function of two currents: the electromagnetic current, in the case of the photon and the weak currents in the case of the weak gauge bosons. The currents are space-like separated, and this separation becomes small as the momentum transfer Q^2 becomes large. This analysis is described in many textbooks. Here we will adopt a different viewpoint, which allows a description of the process that generalizes to other processes involving hadrons at high momentum transfer.

Feynman and Bjorken suggested that we could view the incoming proton as a collection of quarks and gluons, which they collectively referred to as *partons*. They argued that one could define the probability $f_i(x)$ of finding a parton of type i carrying a fraction x of the proton momentum (and similarly for neutrons). At high momentum transfer, they argued that the scattering of the virtual photon (or other particle) off the nucleon would actually involve the scattering of this object off one of the partons, the others being "spectators" (Fig. 3.14). In other words, the cross section for deep inelastic scattering would be given by

$$\begin{aligned}&\sigma(e^-(k)+p(P)\to e^-(k')+X)\\&\quad=\int dx\sum_f f_f(x)\sigma(e^-(k)+q(xP)\to e^-(k')+q_f(p')).\end{aligned}\tag{3.103}$$

This assumption may – should – seem surprising. After all, the scattering process is described by the rules of quantum mechanics and so there should be all sorts of complicated interference effects. We will discuss this question below, but, for now, suffice it to say that the above picture does become correct in QCD for large momentum transfers.

For the case of a virtual photon, the cross section for the parton process can be calculated just as in QED:

$$\frac{d\sigma}{d\hat{t}}(e^-q\to e^-q)=\frac{2\pi\alpha^2Q_f^2}{\hat{s}^2}\left(\frac{\hat{s}^2+\hat{u}^2}{\hat{t}^2}\right).\tag{3.104}$$

Here $\hat{s},\hat{t},\hat{u}$ are the kinematic invariants of the elementary parton process. For example, if we neglect the mass of the lepton and the incoming nucleon:

$$\hat{s}=2p\cdot k=2\zeta P\cdot k=\zeta s.\tag{3.105}$$

https://doi.org/10.1017/9781009290883.008 Published online by Cambridge University Press

If the scattered electron momentum is measured then q is known and we can relate the proton momentum fraction x for the process to measured quantities. From momentum conservation,

$$(\zeta P + q)^2 = 0 \tag{3.106}$$

or

$$q^2 + 2\zeta P \cdot q = 0. \tag{3.107}$$

Solving for ζ:

$$\zeta = x = -\frac{q^2}{2P \cdot q}. \tag{3.108}$$

It is convenient to introduce another kinematic variable,

$$y = \frac{2P \cdot q}{s} = \frac{2P \cdot q}{2P \cdot k}. \tag{3.109}$$

Then $Q^2 = q^2 = xys$, and we can write down the differential cross section:

$$\frac{d^2\sigma}{dxdy}(e^- P \to e^- X) = \left(\sum_f x f_f(x) Q_f^2\right) \frac{2\pi\alpha^2 s}{Q^4}[1 + (1-y)^2]. \tag{3.110}$$

This and related predictions were observed to hold in the first deep inelastic scattering experiments at SLAC, which provided the first persuasive experimental evidence for the reality of quarks. Note, in particular, the scaling implied by these relations. For fixed y the cross section is a function only of x.

In QCD these notions need a crucial refinement. The distribution functions are no longer independent of Q^2:

$$f_f(x) \to f_f(x, Q^2). \tag{3.111}$$

To understand this, we return to the question: why should a probabilistic model of partons work at all in these very quantum processes? Consider, for example, the Feynman diagrams of Fig. 3.15. Clearly there are complicated interference terms when one squares the amplitude. But it turns out that, in certain gauges, the interference diagrams are suppressed and the cross section is just given by the squares of terms, as in Fig. 3.16. So one finds a probabilistic description of the process, just as Feynman and Bjorken suggested, the distribution function being the result of the sequence of interactions in the figure. These diagrams depend on Q^2. One can write integro-differential equations for these functions, the *Altarelli–Parisi equations*. To explain the data, one determines these distribution functions at one value of Q^2 from experiment and then evolves them to other values. By now, the distribution functions have been studied over a broad range of Q^2. The structure functions must be measured at some Q^2; they can then be evolved to higher Q^2. This program has been very successful, as indicated in Fig. 3.17.

https://doi.org/10.1017/9781009290883.008 Published online by Cambridge University Press

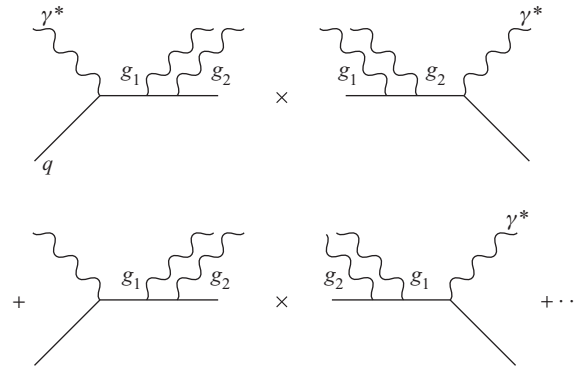

Fig. 3.15 Diagrams contributing to the total rate. The diagrams on the right are complex conjugates of the corresponding amplitudes on the left. The second term represents a complicated interference.

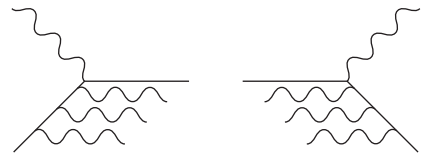

Fig. 3.16 In suitable gauges, deep inelastic scattering is dominated by the absolute squares of amplitudes (interference is unimportant).

3.9.4 Other high-momentum processes

These ideas have been applied to other processes. The analysis which provides a diagrammatic understanding of deep inelastic scattering shows that the same structure functions are relevant to other high-momentum-transfer processes, though care is required in their definitions. Examples include lepton pair production in hadronic collisions (Fig. 3.18) and jet production in hadron collisions, for which a comparison of theory and experiment can be made using Fig. 3.17. But, beyond testing QCD, such processes are crucial to the search for new physics. They have played a critical role in the discovery and study of the Higgs boson and in the exclusion of many possible types of new physics.

3.9.5 QCD beyond the leading order

For many questions it is crucial to compute QCD corrections beyond the leading order. This has been particularly important at the Tevatron and, more recently, the LHC. Such computations present serious challenges, and conventional Feynman diagram analyses are often inadequate. For example, we may be interested in initial states involving two gluons and final states involving two, three, four or more gluons. Already in the computation of the beta function, as discussed in Section 3.5, the three-gluon vertex adds significantly to the algebraic tedium (we avoided some of this by using the background field method).

https://doi.org/10.1017/9781009290883.008 Published online by Cambridge University Press

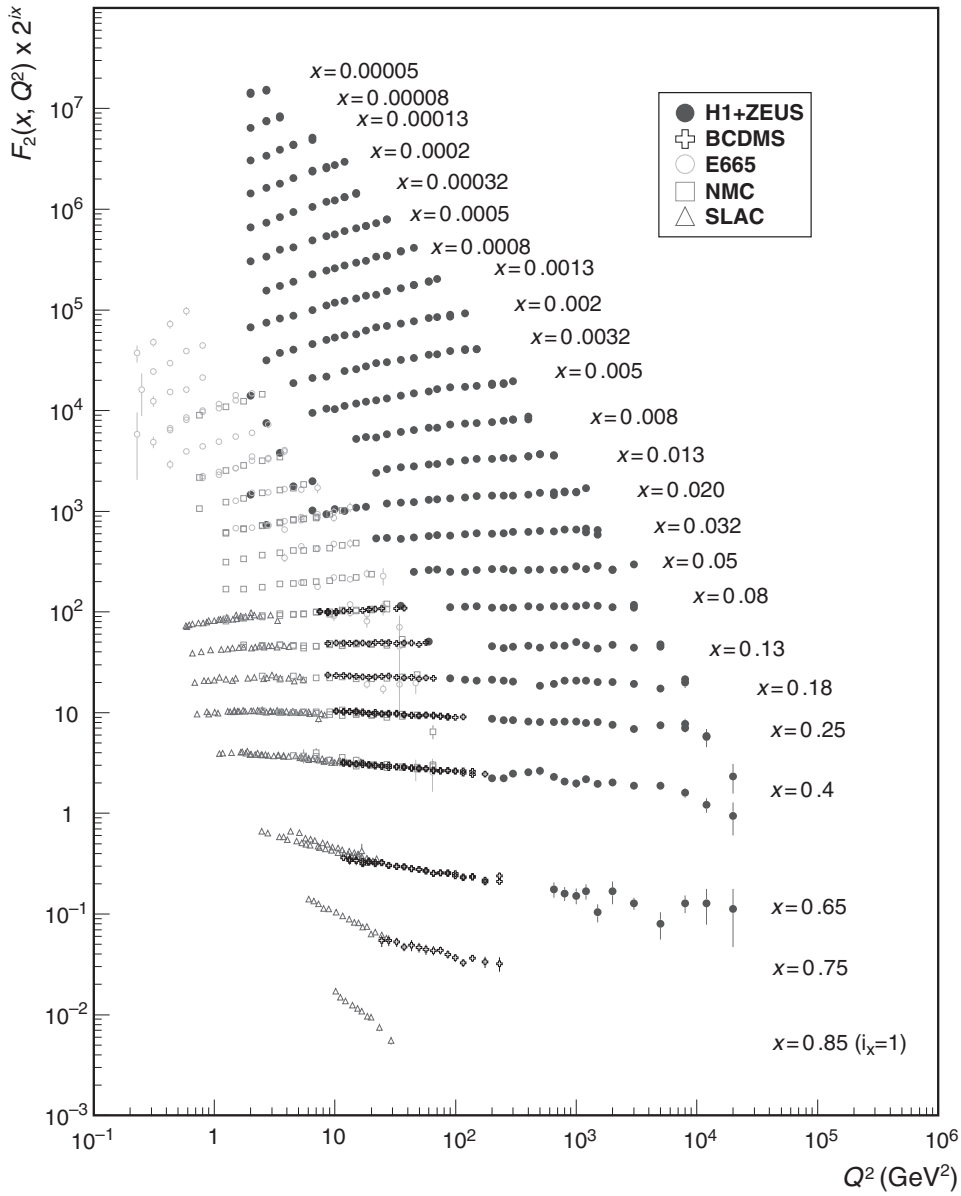

Fig. 3.17 The proton structure function F_2 as a function of Q^2 at fixed x, as determined by several experiments (reproduced by permission of the Particle Data Group).

For cross sections, however, the increase in labor is dramatic, particularly if we follow the standard method of squaring the amplitude and doing polarization and color sums (perhaps with projections). The labor grows essentially exponentially as we add more gluons.Without some cleverness, one quickly exhausts the capabilities of even powerful computers. With the Tevatron, and especially the LHC, programs, the need for such

https://doi.org/10.1017/9781009290883.008 Published online by Cambridge University Press

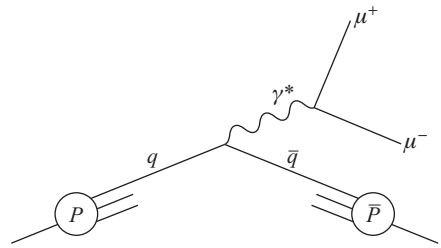

Fig. 3.18 Diagram showing $P\bar{P}$ annihilation with μ-pair production (the Drell–Yan process).

computations, in order to understand the background to possible non-Standard-Model physics has grown dramatically.

Fortunately, there has been significant progress in this arena. A critical aspect of the simplification has been a focus on *amplitudes*, i.e. obtaining the full scattering amplitude before squaring. A simplification of this sort is suggested by string theory, where, as we will see, one computes the scattering amplitude directly and, for example for closed string theories, there is just one diagram at each order. Initially investigators extracted QCD amplitudes from the low-energy limits of such processes, but it soon became clear how to obtain such simplifications directly in field theory. Elements contributing to this progress include the spinor helicity formalism. Here one trades four-vectors for products of spinors. For massless particles these spinors are themselves massless; working with them leads to vast simplifications. Progress in radiative corrections has relied heavily on unitarity, allowing one to compute higher-order diagrams by combining lower-order diagrams. Other important elements include trace-based color descriptions (much as we will see for large N in Chapter 5) and the use of on-shell recursion relations.

Processes involving the collisions of two particles that produce n particles have been calculated at leading order (LO) Amplitudes including one-loop corrections (next to leading order, or NLO) are known for $e^+e^- \to$ seven jets, $pp \to W +$ five jets, $pp \to$ five jets, $W + H$, $H + H$ and $\gamma\gamma$. These computations are now automated and public codes are available, such as GoSam, OpenLoops, Black Hat, Recola and Rocket. Amplitudes including two-loop corrections (NNLO) are known for three-jets production in e^+e^- annihilation and, in pp and $p\bar{p}$ collisions, for the production of Higgs bosons H, $W + H$, $H + H$ and photon pairs.

Suggested reading

There are a number of excellent texts on the Standard Model. *An Introduction to Quantum Field Theory* by Peskin and Schroeder (1995) provides a good introduction both to weak interactions and also to strong interactions, including deep inelastic scattering, parton distributions and the like. Other excellent texts include the books by Cheng and Li (1984), Donoghue *et al*. (1992), Pokorski (2000), Weinberg (1995), Bailin and Love (1993) and Cottingham and Greenwood (1998). More recently Srednicki (2007) and Schwartz (2013)

https://doi.org/10.1017/9781009290883.008 Published online by Cambridge University Press

introduced many of the more modern techniques for calculating QCD amplitudes, and the latter provides a more up-to-date survey of Standard Model computations generally. More detail about QCD amplitudes is presented in the lectures by Dixon (2013), who provides many additional references. An elegant calculation of the beta function in QCD, which uses the Wilson loop to determine the potential perturbatively, appears in the lectures of Susskind (1977). These lectures, as well as Wilson's original paper (1974) and the text of Creutz (1983), provide a good introduction to lattice gauge theory. An important subject which we have not discussed in this chapter is that of heavy-quark physics. This is experimentally important and theoretically accessible. A good introduction is provided in the book by Manohar and Wise (2000). The Particle Data Group website provides excellent reviews about a range of Standard Model (as well as Beyond the Standard Model) topics.

Exercises

(1) Add to the Lagrangian of Eq. (2.41) a term

$$\delta\mathcal{L} = \epsilon \,\mathrm{Tr}\, M \tag{3.112}$$

for small ϵ. Show that, in the presence of ϵ, the expectation values of the $\vec{\pi}$ fields are fixed and have a simple physical explanation. Compute the masses of the $\vec{\pi}$ fields directly from the Lagrangian.

(2) Verify Eqs. (3.48)–(3.56).

(3) Compute the mass of the Higgs field as a function of μ and λ (see Eqs. (2.70), (2.71)). Discuss the production of Higgs particles (you do not need to do detailed calculations, but should indicate the relevant Feynman graphs and make crude estimates at least of the cross sections) in e^+e^-, $\mu^+\mu^-$ and $P\bar{P}$ annihilation. Keep in mind that, because some of the Yukawa couplings are extremely small, there may be processes generated by loop effects that are bigger than processes that arise at tree level.

(4) Using the formula for the e^+e^- cross section, determine the branching ratio for decay of the Z into hadrons:

$$B(Z \to \text{ hadrons}) = \frac{\Gamma(Z \to \text{ hadrons})}{\Gamma(Z \to \text{ all})}. \tag{3.113}$$

https://doi.org/10.1017/9781009290883.008 Published online by Cambridge University Press